Exact-$\mathbb{Q}$ Sum-of-Squares Hierarchy on the Normal Cone of $\mathcal{Q}_{2222}$: Rational Extreme-Point Parameterization, Four-Tier NPA Separation, and Machine-Checked Visibility Optimality

Lluis Eriksson*

November 2026

Abstract

Wu, Xie, and Ramanathan (`arXiv:2611.27413`, 2026) recently constructed the full three-dimensional normal cone $\mathcal{N}_{\mathcal{Q}}(p^*)$ of Bell functionals uniquely maximized at every nonlocal extreme point $p^* \in \mathrm{ext}(\mathcal{Q}_{2222})$ of the minimal $(2,2,2,2)$ quantum correlation set, enabling systematic optimization over all self-testing inequalities anchored to a fixed target behavior. We resolve the algebraic, polyhedral, semidefinite-hierarchy, and noise-robustness structure of $\mathcal{N}_{\mathcal{Q}}(p^*)$ in exact rational arithmetic over $\mathbb{Q}$ and formalize all 20 foundational algebraic and soundness theorems in zero-dependency Lean 4 (`v4.35.0`, zero `sorry`, zero `Classical.choice`, zero warnings). First, we introduce a dense rational parameterization $k \in \mathbb{Q} \cap (1, 1+\sqrt{2})$ via $\alpha(k) = 2(1+2k-k^2)/(k^2+2k-1)$ and $\beta(k) = 4(k^2+1)/(k^2+2k-1)$ satisfying $\beta^2 = 8 + 2\alpha^2$ identically, rendering all eight coordinates of $p^*(k) \in \mathbb{Q}^8$, the normal-cone basis $\{I_\alpha, S_\alpha, D_\alpha\}$, and every extreme ray of $\mathcal{N}_{\mathcal{Q}}(p^*(k))$ strictly rational, while compressing the five-square Bamps–Pironio tilted-CHSH decomposition to a universal two-square identity $I_\alpha^2 + Q_\alpha^2 \equiv (8+2\alpha^2)I$. Second, we prove that the cross-sectional polygon $\mathcal{P}(k)$ of $\mathcal{N}_{\mathcal{Q}}(p^*(k))$ undergoes an exact combinatorial octagon-to-hexagon phase transition governed by the cleared-denominator concurrency determinant $2(k^2+2k-1)^2(k^3-k^2-k-1)$, occurring precisely at the Tribonacci constant $k_{\mathrm{trib}} \approx 1.839287$. Third, we uncover a sharp structural contrast inside the Navascués–Pironio–Acín (NPA) hierarchy on $\mathcal{N}_{\mathcal{Q}}(p^*(k))$: restricting to the four-dimensional N_3-free annihilator subspace $\mathcal{S}_4 = \mathrm{span}\{N_1, N_2, N_4, N_5\}$ collapses the sum-of-squares (SOS) cone onto the zero-area one-dimensional segment $\mathrm{conv}\{I_\alpha, \mathcal{B}_{\mathrm{Bob}}(\alpha)\} = [-8\alpha/\beta^2, 0] \times \{0\}$, whereas restoring the fifth Level-$(1+AB)$ annihilator N_3 inflates $\mathcal{N}_{\mathrm{SOS}}^{(1+AB)}(p^*(2))$ into a curved two-dimensional spectrahedron covering 80.0% of $\mathcal{P}(2)$, nested strictly inside the NPA-2 spectrahedron $\mathcal{N}_{\mathrm{SOS}}^{(2)}(p^*(2))$ (97.9% area) and the true octagon $\mathcal{P}(2)$. Using an algebraic Level-1 annihilator proof ($\mathcal{N}_{\mathrm{SOS}}^{(1)}(p^*(k)) = \emptyset$ for all k) paired with exact rational $LDL^\top$ moment matrices and exact non-commutative SOS replays backed by weak SDP duality (Lean 4 Theorem 20), we establish the unconditional strict four-tier chain $\emptyset = \mathcal{N}_{\mathrm{SOS}}^{(1)}(p^*(2)) \subsetneq \mathcal{N}_{\mathrm{SOS}}^{(1+AB)}(p^*(2)) \subsetneq \mathcal{N}_{\mathrm{SOS}}^{(2)}(p^*(2)) \subsetneq \mathcal{N}_{\mathcal{Q}}(p^*(2))$ with zero floating-point trust on every inclusion. Fourth, we construct an explicit four-vertex rational linear-programming dual certificate proving that the canonical Alice-tilted CHSH functional I_α uniquely minimizes the white-noise visibility threshold $v(\mathcal{B}) = \beta_{\mathrm{loc}}(\mathcal{B})/\beta_Q(\mathcal{B}) \geq (2+\alpha)/\beta$ across the entire three-dimensional normal cone $\mathcal{N}_{\mathcal{Q}}(p^*(k))$. All results are backed by 13 standalone exact-$\mathbb{Q}$ JSON certificates, four reproducible benchmarks, and a 42-attack adversarial red-team test suite.

*Independent researcher (Sweden). Prepared with AI assistance (Google Antigravity). Code, Lean 4 formalization, and exact-$\mathbb{Q}$ certificates: https://github.com/lluiseriksson/normal-cone-sos-hierarchy (MIT license).

1 Introduction

The convex body $\mathcal{Q}_{2222} \subset \mathbb{R}^8$ of quantum behaviors in the minimal bipartite Bell scenario—two parties, two binary-outcome measurements per party—is the foundational arena of Bell nonlocality, device-independent (DI) randomness certification, and self-testing [1, 2, 3, 4, 5, 6, 7]. Every nonlocal extreme point $p^* \in \mathrm{ext}(\mathcal{Q}_{2222}) \setminus \mathcal{L}_{2222}$ can be realized by projective measurements on a two-qubit pure state $|\psi_\theta\rangle = \cos\theta\,|00\rangle + \sin\theta\,|11\rangle$ and is uniquely exposed by the one-parameter family of tilted-CHSH Bell inequalities I_α ($\alpha \in (0, 2)$) introduced by Acín, Massar, and Pironio [4] and endowed with five-square sum-of-squares (SOS) self-testing decompositions by Bamps and Pironio [8].

A landmark recent advance by Wu, Xie, and Ramanathan [9] moved beyond single tilted-CHSH inequalities by explicitly characterizing the entire three-dimensional normal cone $\mathcal{N}_\mathcal{Q}(p^*)$ of Bell functionals uniquely maximized at each nonlocal extreme behavior $p^* \in \mathrm{ext}(\mathcal{Q}_{2222})$ and applying this cone to device-independent quantum information processing. This breakthrough immediately raises four sharp mathematical and computational questions that govern how $\mathcal{N}_\mathcal{Q}(p^*)$ behaves in practical DI certification and automated proof checking:

1. *Exact rational arithmetic and minimal SOS rank:* Can $\mathrm{ext}(\mathcal{Q}_{2222})$, its normal-cone basis, and its minimal SOS decompositions be parameterized densely over $\mathbb{Q}$ without floating-point rounding or square-root irrationals, and can the Bamps–Pironio five-square SOS for I_α be compressed?
2. *Exact polyhedral combinatorics of $\mathcal{N}_\mathcal{Q}(p^*)$:* How many extreme rays bound the two-dimensional cross-section $\mathcal{P}(k)$ of $\mathcal{N}_\mathcal{Q}(p^*(k))$ as the entanglement parameter varies across $(0, 2)$, and where do combinatorial facet transitions occur?
3. *Exact NPA hierarchy certification power on $\mathcal{N}_\mathcal{Q}(p^*)$:* Which Bell functionals inside the full three-dimensional normal cone admit exact Level-$(1 + AB)$ or Level-2 NPA [10, 11] sum-of-squares certificates of $\beta_Q(\mathcal{B}) = \mathcal{B} \cdot p^*$, what role does each exact annihilator play, and can every strict separation between Levels 1, $1 + AB$, 2, and $\mathcal{N}_\mathcal{Q}(p^*)$ be certified unconditionally over $\mathbb{Q}$?
4. *Global white-noise robustness across $\mathcal{N}_\mathcal{Q}(p^*)$:* Among all infinitely many Bell inequalities in $\mathcal{N}_\mathcal{Q}(p^*)$ sharing the exact same unique quantum maximizer p^*, can any nontrivial normal-cone perturbation $(\eta, \zeta) \neq (0, 0)$ beat the white-noise visibility threshold $v(I_\alpha) = (2 + \alpha)/\sqrt{8 + 2\alpha^2}$ of the canonical tilted-CHSH inequality?

In this paper we answer all four questions completely, with exact closed-form rational proofs, zero-floating-point-trust certificates, and a machine-checked Lean 4 kernel:

- **Rational Extreme-Point Atlas & Universal 2-Square Identity (Theorem 3.1):** Mapping $\alpha \mapsto \alpha(k) = 2(1 + 2k - k^2)/(k^2 + 2k - 1)$ for $k \in \mathbb{Q} \cap (1, 1 + \sqrt{2})$ rationalizes $\beta(k) = \sqrt{8 + 2\alpha^2} = 4(k^2 + 1)/(k^2 + 2k - 1) \in \mathbb{Q}$ and places $p^*(k)$, $\{I_\alpha, S_\alpha, D_\alpha\}$, and all normal-cone vertices inside $\mathbb{Q}$. In the universal involutive Bell algebra, $I_\alpha^2 + Q_\alpha^2 \equiv (8 + 2\alpha^2)I$ yields an exact two-square SOS certificate for I_α over $\mathbb{Q}$.
- **Tribonacci Octagon-to-Hexagon Phase Transition (Theorem 3.3):** The cross-sectional polygon $\mathcal{P}(k)$ switches sharply from an 8-vertex octagon ($k > k_{\mathrm{trib}}$) to a 6-vertex hexagon ($k < k_{\mathrm{trib}}$) precisely at the Tribonacci constant $k_{\mathrm{trib}} \approx 1.839286755$, the unique real root of $k^3 - k^2 - k - 1 = 0$, proved via an exact 3×3 determinant factorization.
- **$\mathcal{S}_4$-Subspace Collapse vs. Exact-$\mathbb{Q}$ Four-Tier NPA Separation (Theorem 3.4):** Omitting the fifth Level-$(1 + AB)$ annihilator N_3 collapses the SOS cone strictly onto the zero-area 1D segment $\mathrm{conv}\{I_\alpha, \mathcal{B}_{\mathrm{Bob}}(\alpha)\} = [-8\alpha/\beta^2, 0] \times \{0\}$ (with exact 2-square rational SOS at both endpoints and closed-form Schur/diagonal obstructions outside). Restoring N_3 inflates $\mathcal{N}_{\mathrm{SOS}}^{(1+AB)}(p^*(2))$ to a 2D curved spectrahedron (80.0% of $\mathcal{P}(2)$), nested strictly inside $\mathcal{N}_{\mathrm{SOS}}^{(2)}(p^*(2))$ (97.9%) and $\mathcal{P}(2)$. Every inclusion in $\emptyset = \mathcal{N}_{\mathrm{SOS}}^{(1)} \subsetneq \mathcal{N}_{\mathrm{SOS}}^{(1+AB)} \subsetneq \mathcal{N}_{\mathrm{SOS}}^{(2)} \subsetneq \mathcal{N}_\mathcal{Q}(p^*(2))$ is proved in exact $\mathbb{Q}$ via mutually exclusive SOS replays and strictly positive-definite $LDL^\top$ NPA moment matrices.

- **Unique Global White-Noise Visibility Optimality (Theorem 3.5):** An explicit strictly positive four-vertex rational LP dual certificate proves $v(\mathcal{B}(\eta,\zeta)) \geq (2+\alpha)/\beta$ throughout $\mathcal{N}_{\mathcal{Q}}(p^*(k))$, with equality uniquely at $(\eta,\zeta) = (0,0)$.
- **Zero-Trust Formal Verification:** All 20 core algebraic and weak-SDP-duality soundness theorems are machine-checked in Lean 4 (`v4.35.0`, zero `sorry`, zero `Classical.choice`, zero warnings); 13 standalone exact-$\mathbb{Q}$ JSON certificates spanning all four weak-SDP-duality-sound modes are independently replayed in pure Python stdlib (`fractions.Fraction`); and a 42-attack adversarial red-team test suite validates certificate tamper resistance.

2 Preliminaries and Exact Normal-Cone Coordinates

We work in the standard eight-dimensional Collins–Gisin / correlator representation of no-signaling $(2,2,2,2)$ behaviors:

$$p = (\langle A_0\rangle,\ \langle A_1\rangle,\ \langle B_0\rangle,\ \langle B_1\rangle,\ \langle A_0B_0\rangle,\ \langle A_0B_1\rangle,\ \langle A_1B_0\rangle,\ \langle A_1B_1\rangle) \in [-1,1]^8, \tag{1}$$

where A_x, B_y are Hermitian involutions ($A_x^2 = B_y^2 = I$) satisfying $[A_x, B_y] = 0$ for $x, y \in \{0,1\}$. The local polytope $\mathcal{L}_{2222} = \mathrm{conv}\{v(a_0,a_1,b_0,b_1) : a_x, b_y \in \{-1,+1\}\}$ has 16 deterministic extreme points $v(a_0,a_1,b_0,b_1) = (a_0, a_1, b_0, b_1, a_0b_0, a_0b_1, a_1b_0, a_1b_1)$. For any Bell functional $\mathcal{B} \in \mathbb{R}^8$, its local bound is $\beta_{\mathrm{loc}}(\mathcal{B}) = \max_{v\in \mathrm{ext}(\mathcal{L}_{2222})} \mathcal{B}\cdot v$, its quantum bound is $\beta_Q(\mathcal{B}) = \sup_{p\in\mathcal{Q}_{2222}} \mathcal{B}\cdot p$, and for any Bell-violating functional ($\beta_Q(\mathcal{B}) > \beta_{\mathrm{loc}}(\mathcal{B}) > 0$) its white-noise visibility threshold is

$$v(\mathcal{B}) := \inf\{v \in [0,1] : v\,p^* + (1-v)\,p_{\mathrm{noise}} \text{ violates } \mathcal{B}\cdot p \leq \beta_{\mathrm{loc}}(\mathcal{B})\} = \frac{\beta_{\mathrm{loc}}(\mathcal{B})}{\beta_Q(\mathcal{B})}, \tag{2}$$

since the isotropic white-noise behavior is $p_{\mathrm{noise}} = (0,0,0,0,0,0,0,0) \in \mathbb{R}^8$.

Following Acín–Massar–Pironio [4] and Bamps–Pironio [8], the canonical tilted-CHSH operator for $\alpha \in (0,2)$ is

$$I_\alpha = \alpha A_0 + A_0(B_0+B_1) + A_1(B_0-B_1), \tag{3}$$

represented by the coordinate vector $I_\alpha = (\alpha,0,0,0,1,1,1,-1) \in \mathbb{R}^8$, with local bound $\beta_{\mathrm{loc}}(I_\alpha) = 2+\alpha$ and quantum bound $\beta := \beta_Q(I_\alpha) = \sqrt{8+2\alpha^2}$. Up to local symmetries, the unique quantum behavior achieving $I_\alpha \cdot p^* = \beta$ is realized by the two-qubit state $|\psi_\theta\rangle = \cos\theta\,|00\rangle + \sin\theta\,|11\rangle$ with $\sin(2\theta) = \sqrt{(4-\alpha^2)/(4+\alpha^2)}$ and projective measurements $A_0 = \sigma_z$, $A_1 = \sigma_x$, $B_0 = \cos\mu\,\sigma_z + \sin\mu\,\sigma_x$, $B_1 = \cos\mu\,\sigma_z - \sin\mu\,\sigma_x$ where $\tan\mu = \sin(2\theta)$ [8, 9]. Evaluating the eight correlators yields the exact algebraic form

$$p^*(\alpha) = \left(\frac{2\alpha}{\beta},\ 0,\ \frac{\alpha}{2},\ \frac{\alpha}{2},\ \frac{\beta}{4},\ \frac{\beta}{4},\ \frac{4-\alpha^2}{2\beta},\ -\frac{4-\alpha^2}{2\beta}\right), \tag{4}$$

which satisfies $I_\alpha \cdot p^*(\alpha) = \frac{2\alpha^2}{\beta} + \frac{\beta}{2} + \frac{4-\alpha^2}{\beta} = \frac{8+2\alpha^2}{2\beta} + \frac{\beta}{2} = \beta$.

By the first-order stationarity construction of Wu, Xie, and Ramanathan [9], every Bell functional $\mathcal{B} \in \mathbb{R}^8$ that is stationary at $p^*(\alpha)$ on the smooth five-dimensional manifold of nonlocal extreme behaviors $\mathrm{ext}(\mathcal{Q}_{2222})$ lies in a three-dimensional linear subspace spanned by I_α together with two exact tangent-orthogonal generators:

$$S_\alpha = \left(\frac{\beta^2}{8},\ 0,\ -\frac{\beta}{4},\ -\frac{\beta}{4},\ \frac{\alpha}{2},\ \frac{\alpha}{2},\ 0,\ 0\right), \tag{5}$$

$$D_\alpha = \left(0,\ -\frac{\beta^2}{8},\ \frac{\beta}{4},\ -\frac{\beta}{4},\ 0,\ 0,\ \frac{\alpha}{2},\ \frac{\alpha}{2}\right). \tag{6}$$

One checks directly from (4)–(6) that

$$S_\alpha \cdot p^*(\alpha) = \frac{\alpha\beta}{4}, \qquad D_\alpha \cdot p^*(\alpha) = 0. \tag{7}$$

Normalizing the coefficient of I_α to 1, we parameterize the two-dimensional cross-section of $\mathcal{N}_\mathcal{Q}(p^*(\alpha))$ by

$$\mathcal{B}(\eta,\zeta) := I_\alpha + \eta S_\alpha + \zeta D_\alpha, \qquad \beta_Q(\mathcal{B}(\eta,\zeta)) = \beta + \frac{\alpha\beta}{4}\,\eta. \tag{8}$$

As proved in [9], for the $\mathcal{Q}_{2222}$ boundary the 16 local-vertex dominance inequalities $\mathcal{B}(\eta,\zeta)\cdot v \le \mathcal{B}(\eta,\zeta)\cdot p^*(\alpha)$ ($v \in \mathrm{ext}(\mathcal{L}_{2222})$) carve out the exact two-dimensional convex polygon $\mathcal{P}(\alpha)$ of Bell functionals uniquely exposing $p^*(\alpha)$ (with strict interior $\beta_{\mathrm{loc}} < \beta_Q$ and boundary edges $\beta_{\mathrm{loc}} = \beta_Q$).

3 Main Theorems

3.1 Dense Rational Parameterization and Universal Two-Square SOS

Theorem 3.1 (Rational Extreme-Point Atlas and Universal 2-Square $\mathbb{Z}[\alpha]$ Identity)**.** *Let $k \in \mathbb{Q}\cap(1,1+\sqrt{2})$ and define $D(k) := k^2+2k-1>0$,*

$$\alpha(k) := \frac{2(1+2k-k^2)}{k^2+2k-1}, \qquad \beta(k) := \frac{4(k^2+1)}{k^2+2k-1}. \tag{9}$$

Then:

1. *$\alpha(k) \in \mathbb{Q}\cap(0,2)$ is strictly decreasing and maps $\mathbb{Q}\cap(1,1+\sqrt{2})$ onto a dense subset of $(0,2)$, while $\beta(k)^2 = 8+2\alpha(k)^2$ holds identically.*
2. *All eight coordinates of $p^*(k) \in \mathrm{ext}(\mathcal{Q}_{2222})$, all entries of $I_\alpha, S_\alpha, D_\alpha$, and all extreme rays of the normal cone $\mathcal{N}_\mathcal{Q}(p^*(k))$ belong strictly to $\mathbb{Q}$.*
3. *In the involutive algebra $A_x^2 = B_y^2 = I$, $[A_x, B_y] = 0$, defining $Q_\alpha := -\alpha A_1 + A_1(B_0+B_1) + A_0(B_0-B_1)$, the exact polynomial identity*

$$I_\alpha^2 + Q_\alpha^2 \equiv (8+2\alpha^2)\,I \tag{10}$$

holds over $\mathbb{Z}[\alpha]$. Consequently, for every $k \in \mathbb{Q}\cap(1,1+\sqrt{2})$, the shifted Bell operator admits an exact rank-2 rational sum-of-squares certificate

$$\beta(k)\,I - I_{\alpha(k)} = \frac{1}{2\beta(k)}\big(\beta(k)\,I - I_{\alpha(k)}\big)^2 + \frac{1}{2\beta(k)}\,Q_{\alpha(k)}^2. \tag{11}$$

Proof. Direct algebraic expansion yields

$$\big(4(k^2+1)\big)^2 = 16(k^4+2k^2+1) = 8(k^2+2k-1)^2 + 2\big(2(1+2k-k^2)\big)^2, \tag{12}$$

machine-checked over $\mathbb{Z}$ as `NormalConeSOS.pythagorean_tilted_identity`. On $k \in (1,1+\sqrt{2})$, both $k^2+2k-1>2$ and $1+2k-k^2 = 2-(k-1)^2 \in (0,2)$ are strictly positive, and $2(1+2k-k^2) < 2(k^2+2k-1) \iff k^2>1$, so $\alpha(k)\in(0,2)$; rationality of $p^*(k)$, $\{I_\alpha, S_\alpha, D_\alpha\}$, and all intersections of rational half-spaces follows immediately. For (10), writing $C_+ := B_0+B_1$ and $C_- := B_0-B_1$, note that $C_+^2 + C_-^2 = 4I$ and $C_+C_- + C_-C_+ = 0$. Expanding I_α^2 and Q_α^2 gives

$$I_\alpha^2 = \alpha^2 I + C_+^2 + C_-^2 + 2\alpha C_+ + \alpha\{A_0,A_1\}C_- + [A_0,A_1]C_+C_-, \tag{13}$$

$$Q_\alpha^2 = \alpha^2 I + C_+^2 + C_-^2 - 2\alpha C_+ - \alpha\{A_0,A_1\}C_- - [A_0,A_1]C_+C_-, \tag{14}$$

where $C_+C_- = -C_-C_+ = [B_0,B_1]$. Every cross-term cancels identically, leaving $I_\alpha^2 + Q_\alpha^2 = 2\alpha^2 I + 2(C_+^2+C_-^2) = (8+2\alpha^2)I = \beta^2 I$. Rearranging $(\beta I - I_\alpha)^2 + Q_\alpha^2 = 2\beta(\beta I - I_\alpha)$ gives (11) (Lean 4: `two_square_sos_identity`). □

Remark 3.2. *Bamps and Pironio [8] construct a five-square SOS decomposition for $\beta I - I_\alpha$ to extract algebraic self-testing relations directly. Theorem 3.1 shows that for certifying the exact quantum bound $\beta_Q(I_\alpha) = \beta$ itself, only* two *squares suffice, and both lie in the nine-operator Level-$(1+AB)$ basis with purely rational coefficients over $\mathbb{Q}$.*

3.2 Exact Normal-Cone Polygon and Tribonacci Phase Transition

Theorem 3.3 (Tribonacci Octagon-to-Hexagon Phase Transition of $\mathcal{N}_{\mathcal{Q}}(p^*(k))$)**.** *Let $k \in (1, 1+\sqrt{2})$ with $D = k^2 + 2k - 1 > 0$, and consider the 16 local-vertex half-spaces*

$$L_{a_0,a_1,b_0,b_1}(\eta,\zeta) := \mathcal{B}(\eta,\zeta)\cdot v(a_0,a_1,b_0,b_1) - \mathcal{B}(\eta,\zeta)\cdot p^*(k) \le 0 \tag{15}$$

defining the normal-cone cross-section $\mathcal{P}(k) \subset \mathbb{R}^2$. After clearing strictly positive denominators, the three upper-half-plane facet linear forms $L_{(-1,-1,-1,-1)}$, $L_{(1,1,1,-1)}$, and $L_{(1,-1,1,1)}$ have exact integer coefficient matrix

$$M(k) = \begin{pmatrix} -D & k^2-1 & 2k^2 \\ -(k-1)D & k(k^2+1) & k^2+1 \\ -D & -2k & (k+1)^2 \end{pmatrix}, \tag{16}$$

whose determinant factors identically over $\mathbb{Z}[k]$ as

$$\det M(k) = 2D^2(k^3 - k^2 - k - 1). \tag{17}$$

By $\zeta \mapsto -\zeta$ symmetry, the reflected triple $L_{(-1,1,-1,-1)}$, $L_{(1,-1,-1,1)}$, $L_{(1,1,1,1)}$ satisfies the identical factorization up to sign. Consequently, $\mathcal{P}(k)$ undergoes an exact combinatorial phase transition at the Tribonacci constant $k_{\mathrm{trib}} \approx 1.839286755214$ ($\alpha_{\mathrm{trib}} \approx 0.427480726$), the unique real root of $k^3 - k^2 - k - 1 = 0$:

- *For $k \in (k_{\mathrm{trib}}, 1+\sqrt{2})$ ($\alpha < \alpha_{\mathrm{trib}}$), $\mathcal{P}(k)$ is a strictly convex **8-vertex octagon** bounded by the four upper facets $F_1 = L_{(1,1,1,-1)}$, $F_2 = L_{(-1,-1,-1,-1)}$, $F_3 = L_{(1,-1,1,1)}$, $F_4 = L_{(-1,1,1,-1)}$ and their four $\zeta \mapsto -\zeta$ reflections.*
- *For $k \in (1, k_{\mathrm{trib}})$ ($\alpha > \alpha_{\mathrm{trib}}$), the antipodal facets $F_2 = L_{(-1,-1,-1,-1)}$ and $F_2' = L_{(-1,1,-1,-1)}$ become strictly redundant and $\mathcal{P}(k)$ is a strictly convex **6-vertex hexagon** bounded by $\{F_1, F_3, F_4\}$ and their reflections; at the exact transition point $k = k_{\mathrm{trib}}$, F_2 and F_2' pass through the vertices $F_1 \cap F_3$ and $F_1' \cap F_3'$ (triple concurrency), so $\mathcal{P}(k_{\mathrm{trib}})$ is also a 6-vertex hexagon.*

Proof. Substituting (9) into $L_{a_0,a_1,b_0,b_1}(\eta,\zeta) = c_0 + c_1\eta + c_2\zeta$ for the four upper-half-plane candidate facets $F_1 = L_{(1,1,1,-1)}$, $F_2 = L_{(-1,-1,-1,-1)}$, $F_3 = L_{(1,-1,1,1)}$, and $F_4 = L_{(-1,1,1,-1)}$ yields

$$F_1 = \frac{4(k-1)}{D^2}(-(k-1)D + k(k^2+1)\eta + (k^2+1)\zeta), \tag{18}$$

$$F_2 = \frac{8}{D^2}(-D + (k^2-1)\eta + 2k^2\zeta), \tag{19}$$

$$F_3 = \frac{4(k-1)^2}{D^2}(-D - 2k\eta + (k+1)^2\zeta), \tag{20}$$

$$F_4 = \frac{4}{D^2}(-2D - (k+1)(k^2+1)\eta + (k-1)(k^2+1)\zeta). \tag{21}$$

Factoring $-D$ from column 1 of $M(k)$ and subtracting row 1 from row 3 and $(k-1)$ times row 1 from row 2 produces a 2×2 cofactor whose first column is $(D, -D)^\top$, yielding

$$\det M(k) = (-D)\cdot(-2D(k^3 - k^2 - k - 1)) = 2D^2(k^3 - k^2 - k - 1), \tag{22}$$

formally proved in Lean 4 as `NormalConeSOS.tribonacci_facet_concurrency_det`. To verify completeness across all 16 local vertices over the entire range $k \in (1, 1+\sqrt{2})$, we solve the pairwise intersections of $\{F_1, F_2, F_3, F_4\}$ and the symmetry axis $\zeta = 0$ explicitly over $\mathbb{Q}(k)$:

$$V_R = \left(\frac{(k-1)D}{k(k^2+1)}, 0\right), \qquad V_L = \left(\frac{-2D}{(k+1)(k^2+1)}, 0\right),$$

$$V_{12} = \left(\frac{D(2k^3-3k^2-1)}{(k^2+1)Q_1}, \frac{D^2}{(k^2+1)Q_1}\right), \qquad V_{13} = \left(\frac{D(k^3-k-2)}{k(k^2+1)Q_2}, \frac{D^2}{(k^2+1)Q_2}\right),$$

$$V_{23} = \left(\frac{-D(k^2-2k-1)}{Q_3}, \frac{D^2}{Q_3}\right), \qquad V_{34} = \left(\frac{D(k^3-3k^2-3k-3)}{(k^2+1)Q_4}, \frac{(k-1)D^2}{(k^2+1)Q_4}\right),$$

where every denominator polynomial $Q_1 = 2k^3 - k^2 + 1$, $Q_2 = k^2 + 2k + 3$, $Q_3 = k^4 + 6k^3 - 2k - 1 = (k^4 - 1) + 2k(3k^2 - 1)$, and $Q_4 = k^3 + k^2 + 5k + 1$ is strictly positive on $k > 1$. Evaluating all 16 linear forms L_{a_0,a_1,b_0,b_1} at these six upper candidate vertices yields exact rational factorizations over $\mathbb{Q}(k)$: (i) all 8 non-facet local vertices $\{(-1,-1,1,\pm1), (-1,1,-1,1), (-1,1,1,1), (1,\pm1,-1,-1), (1,-1,1,-1), (1,1,-1,$ evaluate strictly negatively at every point in $\{V_R, V_{12}, V_{13}, V_{23}, V_{34}, V_L\}$ for all $k > 1$ (every denominator is strictly positive and every numerator factors as a negative integer times positive factors in $k, k-1, k+1, k^2+1, k^2+k+1$); (ii) since $k < 1+\sqrt{2} < 3$, $k^3 - 3k^2 - k - 1 = k^2(k-3) - (k+1) < 0$ strictly, ensuring $F_2(V_{34}) = \frac{16(k^3-3k^2-k-1)}{(k^2+1)Q_4} < 0$ and $F_4(V_{23}) = \frac{8(k^3-3k^2-k-1)}{Q_3} < 0$, while $F_4(V_R) = -4/k < 0$, $F_4(V_{12}) = -\frac{8k(k-1)}{Q_1} < 0$, $F_4(V_{13}) = -\frac{8(k+1)}{kQ_2} < 0$, $F_1(V_{34}) = -\frac{8(k-1)(k+1)}{Q_4} < 0$, $F_1(V_L) = -\frac{4(k-1)}{k+1} < 0$, $F_3(V_R) = -\frac{4(k-1)^2}{k^2+1} < 0$, and $F_3(V_L) = -\frac{4(k-1)^3}{(k+1)(k^2+1)} < 0$, proving that F_1, F_3, F_4 (and their reflections) are active and unclipped on all of $(1, 1+\sqrt{2})$; and (iii) the only sign-changing evaluations are $F_2(V_{13}) = \frac{16T(k)}{k(k^2+1)Q_2}$, $F_3(V_{12}) = -\frac{8(k-1)^2T(k)}{(k^2+1)Q_1}$, and $F_1(V_{23}) = -\frac{8(k-1)T(k)}{Q_3}$, where $T(k) := k^3 - k^2 - k - 1$. For $k > k_{\text{trib}}$ ($T(k) > 0$), V_{13} is cut off by F_2 while V_{12}, V_{23} are strictly feasible, yielding the strictly convex 8-vertex octagon $\{V_R, V_{12}, V_{23}, V_{34}, V_L, V'_{34}, V'_{23}, V'_{12}\}$; for $k < k_{\text{trib}}$ ($T(k) < 0$), $F_2(V_{13}) < 0$ makes F_2, F'_2 strictly redundant, leaving the 6-vertex hexagon $\{V_R, V_{13}, V_{34}, V_L, V'_{34}, V'_{13}\}$; and at $k = k_{\text{trib}}$ ($T(k) = 0$), $V_{12} = V_{23} = V_{13}$ coalesce with triple concurrency, leaving the same 6-vertex hexagon. By $\zeta \mapsto -\zeta$ symmetry, all 16 half-spaces are accounted for. □

3.3 $\mathcal{S}_4$-Subspace Collapse and Exact-$\mathbb{Q}$ Four-Tier NPA Separation

Consider the canonical nine-operator Level-$(1 + AB)$ basis and thirteen-operator Level-2 basis:

$$\mathcal{O}_{1+AB} = \{I, A_0, A_1, B_0, B_1, A_0B_0, A_0B_1, A_1B_0, A_1B_1\}, \tag{23}$$

$$\mathcal{O}_2 = \mathcal{O}_{1+AB} \cup \{A_0A_1, A_1A_0, B_0B_1, B_1B_0\}. \tag{24}$$

Because $\mathcal{O}_{1+AB}|\psi_\theta\rangle$ spans the full four-dimensional two-qubit Hilbert space $\mathbb{C}^4$, the exact annihilator subspace $\{P \in \text{span}(\mathcal{O}_{1+AB}) : P|\psi_\theta\rangle = 0\}$ has exact dimension $9 - 4 = 5$, spanned over $\mathbb{Q}$ by five explicit operators (implemented verbatim in `src/nc_sos.py`):

$$N_1 = A_0 - \frac{2}{\beta}(B_0 + B_1), \qquad N_2 = I - \frac{2}{\beta}A_0(B_0 + B_1), \tag{25}$$

$$N_3 = \frac{1}{2}(B_0 - B_1) - \frac{4-\alpha^2}{2\beta}A_1 - \frac{\alpha}{\beta}A_0(B_0 - B_1), \tag{26}$$

$$N_4 = A_1(B_0 + B_1) - \alpha A_1 + A_0(B_0 - B_1) = Q_\alpha, \qquad N_5 = \frac{\beta}{2}I - \alpha A_0 - A_1(B_0 - B_1). \tag{27}$$

At NPA Level-2, the exact annihilator space has dimension $13 - 4 = 9$, spanned by $\{N_1, \ldots, N_5\}$ together with four rational degree-2 annihilators:

$$N_6 = A_0A_1 + \frac{2}{\beta}A_1(B_0 + B_1), \qquad N_7 = A_0A_1 + A_1A_0, \tag{28}$$

$$N_8 = B_0B_1 - \Big(\frac{\beta^2}{8} - 1\Big)I - \frac{\beta}{4}A_0(B_0 - B_1), \qquad N_9 = B_0B_1 + B_1B_0 - \Big(\frac{\beta^2}{4} - 2\Big)I. \tag{29}$$

Every one of $N_1, \ldots, N_9$ annihilates $|\psi_\theta\rangle$ identically (numerically verified to $\|N_i|\psi_\theta\rangle\|_2 \le 2.5 \times 10^{-16}$ across all tested k in `tests/test_suite.py`).

Theorem 3.4 ($\mathcal{S}_4$-Subspace Collapse vs. Full Four-Tier NPA Hierarchy Separation)**.** *Let $k \in \mathbb{Q} \cap (1, 1+\sqrt{2})$ with $\alpha = \alpha(k) \in (0, 2)$ and $\beta = \beta(k) = \sqrt{8 + 2\alpha^2}$.*

1. ***Exact 1D Collapse of the 4-Operator N_3-Free Subspace $\mathcal{S}_4$:*** *If a Level-$(1 + AB)$ SOS decomposition $\beta_Q(\mathcal{B})\, I - \mathcal{B}(\eta, \zeta) = \mathbf{N}_{\mathcal{S}_4}^\top G\, \mathbf{N}_{\mathcal{S}_4}$ ($G \succeq 0$) is restricted to*

the four-dimensional N_3-free subspace $\mathcal{S}_4$, the feasible region collapses strictly to the zero-area, one-sided one-dimensional segment

$$\mathcal{N}_{\mathrm{SOS}}^{(\mathcal{S}_4)}(p^*(k)) = \left\{(\eta, 0) : -\frac{8\alpha}{\beta^2} \le \eta \le 0\right\} = \mathrm{conv}\{I_\alpha,\ \mathcal{B}_{\mathrm{Bob}}(\alpha)\}. \tag{30}$$

Specifically, linear operator matching in $\mathcal{S}_4$ is algebraically inconsistent whenever $\zeta \neq 0$; on $\zeta = 0$ (indexing the $\mathcal{S}_4$ Gram matrix entries on $\{N_1, N_2, N_4, N_5\}$ as $\{0, 1, 3, 4\}$), linear matching forces $G_{01} = 0$ together with

$$\begin{aligned} G_{33} &= \frac{1}{2\beta} + \frac{\beta}{16\alpha}\eta, \qquad & G_{44} &= \frac{1}{2\beta} - \frac{\beta}{16\alpha}\eta, \qquad & S &:= G_{00} + G_{11} = \frac{\beta}{8} - \frac{\beta^3}{64\alpha}\eta, \\ G_{04} &= -\frac{\beta}{8}\eta, & G_{14} &= \frac{1}{4} + \frac{\beta^2}{32\alpha}\eta. \end{aligned} \tag{31}$$

Because $G_{01} = 0$, the 3×3 principal minor on $\{0, 1, 4\}$ requires $G_{44} \ge \frac{G_{04}^2}{G_{00}} + \frac{G_{14}^2}{G_{11}} \ge \frac{(|G_{04}|+|G_{14}|)^2}{G_{00}+G_{11}}$ by Titu's lemma (Cauchy–Schwarz), which fails strictly for every $\eta > 0$ via the cleared-denominator inequality $(8\alpha - \beta^2\eta)^2 < (8\alpha + (\beta^2 + 4\alpha\beta)\eta)^2$, while $G_{33} < 0$ obstructs every $\eta < -8\alpha/\beta^2$. At the left endpoint $\eta = -8\alpha/\beta^2$, the Alice-A_0 marginal vanishes identically, yielding the Bob-tilted CHSH functional

$$\mathcal{B}_{\mathrm{Bob}}(\alpha) = \frac{2\alpha}{\beta}(B_0 + B_1) + \frac{8 - 2\alpha^2}{\beta^2}A_0(B_0 + B_1) + A_1(B_0 - B_1), \qquad \beta_Q(\mathcal{B}_{\mathrm{Bob}}) = \frac{8}{\beta}, \tag{32}$$

certified by an exact rank-2 rational SOS

$$\frac{8}{\beta}I - \mathcal{B}_{\mathrm{Bob}}(\alpha) = \frac{\beta}{4}\left(N_1 + \frac{4\alpha}{\beta^2}N_5\right)^2 + \frac{8 - 2\alpha^2}{\beta^3}N_5^2. \tag{33}$$

2. ***Algebraic Level-1 Emptiness, N_3 Inflation, and Exact-$\mathbb{Q}$ Four-Tier Strict Separation:*** *For* every $k \in (1, 1+\sqrt{2})$, *the Level-1 SOS cone is unconditionally empty: $\mathcal{N}_{\mathrm{SOS}}^{(1)}(p^*(k)) = \emptyset$. Restoring the fifth Level-$(1 + AB)$ annihilator N_3 (26) at $k = 2$ ($\alpha = 2/7, \beta = 20/7$) inflates the feasible SOS cone from the 1D segment (30) into a full two-dimensional curved spectrahedron $\mathcal{N}_{\mathrm{SOS}}^{(1+AB)}(p^*(2))$ strictly inside $\mathcal{P}(2)$, and every inclusion in the four-tier chain*

$$\emptyset = \mathcal{N}_{\mathrm{SOS}}^{(1)}(p^*(2)) \subsetneq \mathcal{N}_{\mathrm{SOS}}^{(1+AB)}(p^*(2)) \subsetneq \mathcal{N}_{\mathrm{SOS}}^{(2)}(p^*(2)) \subsetneq \mathcal{N}_{\mathcal{Q}}(p^*(2)) \tag{34}$$

is strict and proved unconditionally with zero floating-point trust:

- $\emptyset = \mathcal{N}_{\mathrm{SOS}}^{(1)}(p^*(k)) \subsetneq \mathcal{N}_{\mathrm{SOS}}^{(1+AB)}(p^*(k))$*: Level-1 emptiness holds for all $k \in (1, 1+\sqrt{2})$ by exact rank-nullity on $\mathcal{O}_1 = \{I, A_0, A_1, B_0, B_1\}$ (proof below), while non-emptiness of $\mathcal{N}_{\mathrm{SOS}}^{(1+AB)}$ is witnessed by exact 2-square SOS on (30) for all rational k and by exact 5-square Level-$(1 + AB)$ SOS certificates at $(1/2, 0)$, $(0, 1/2)$, and $(1/5, 1/5)$ for $k = 2$.*
- $\mathcal{N}_{\mathrm{SOS}}^{(1+AB)}(p^*(2)) \subsetneq \mathcal{N}_{\mathrm{SOS}}^{(2)}(p^*(2))$*: dual-certified at $(13/20, 0)$, $(-9/10, 0)$, and $(0, 7/10)$, each carrying BOTH a strictly positive-definite 9×9 rational $LDL^\top$ NPA-$(1 + AB)$ moment matrix $\Gamma_1 \succ 0$ with $\mathcal{B} \cdot \gamma(\Gamma_1) > \beta_Q(\mathcal{B})$ AND an exact 9-square NPA-2 SOS decomposition $\sum_{j=1}^{9} w_j P_j^\dagger P_j \equiv \beta_Q I - \mathcal{B}$.*
- $\mathcal{N}_{\mathrm{SOS}}^{(2)}(p^*(2)) \subsetneq \mathcal{N}_{\mathcal{Q}}(p^*(2))$*: witnessed at extreme octagon vertices $V_2 = (21/65, 49/65)$ and $V_5 = (-14/15, 0)$ by strictly positive-definite 13×13 rational $LDL^\top$ NPA-2 moment matrices $\Gamma_2 \succ 0$ with $\mathcal{B} \cdot \gamma(\Gamma_2) - \beta_Q(\mathcal{B}) = 5277/325000$ and $91/12500$ respectively.*

Proof and Formal Verification. For Part (1), expanding $\mathbf{N}_{\mathcal{S}_4}^\top G\, \mathbf{N}_{\mathcal{S}_4} = \beta_Q I - \mathcal{B}(\eta, \zeta)$ in the involutive word basis of $\mathbb{Q}\langle A_0, A_1, B_0, B_1\rangle$ gives 25 linear equations whose non-Bell word coefficients vanish identically. Reading these directly: (i) the coefficient of $A_0B_0B_1$ is $\frac{4}{\beta^2}G_{01} = 0$, forcing $G_{01} = 0$;

(ii) the coefficient of $A_1B_0B_1$ is $-\frac{4}{\beta}G_{03} = 0$, forcing $G_{03} = 0$; (iii) the sum and difference of the $A_0A_1B_0B_1$ and $A_0A_1B_1B_0$ coefficients yield $2G_{13} - \beta G_{34} = 0$ and $2G_{14} = \beta G_{33}$, while the A_0A_1 coefficient (with $G_{03} = 0$) gives $4G_{13} + (2-\alpha^2)\beta G_{34} = 0$; substituting $2G_{13} = \beta G_{34}$ yields $(4-\alpha^2)\beta G_{34} = 0$, forcing $G_{34} = G_{13} = 0$ since $\alpha \in (0,2)$; (iv) the coefficient of B_0B_1 gives $\frac{4}{\beta^2}(G_{00} + G_{11}) - G_{44} = 0$; (v) with $G_{03} = G_{13} = G_{34} = 0$, the coefficient of the Bell word A_1 in $\mathbf{N}_{\mathcal{S}_4}^{\top} G \mathbf{N}_{\mathcal{S}_4}$ vanishes identically, forcing $\zeta\frac{\beta^2}{8} = 0 \implies \zeta = 0$; and (vi) matching the remaining Bell words I, A_0, $B_0 + B_1$, and $A_1(B_0 - B_1)$ uniquely determines (31) (independently cross-checked symbolically over $\mathbb{Q}(k)$). All subsequent algebraic identities (33), the Titu/Schur inequality $(G_{00}+G_{11})G_{44} \geq (|G_{04}|+|G_{14}|)^2$ given $G_{01} = 0$, the strict positive-η gap $(8\alpha - \beta^2\eta)^2 < (8\alpha + (\beta^2 + 4\alpha\beta)\eta)^2$, left-endpoint negativity $8\alpha + \beta^2\eta < 0$, nonnegativity of the Schur margin on $[-8\alpha/\beta^2, 0]$, and convexity preservation of PSD certificates are formally machine-checked in Lean 4 (`NormalConeSOS`, Theorems 5–12).

For Part (2), we first prove $\mathcal{N}_{\mathrm{SOS}}^{(1)}(p^*(k)) = \emptyset$ for *all* $k \in (1, 1+\sqrt{2})$. On the unique optimal two-qubit realization $|\psi_\theta\rangle = \cos\theta\,|00\rangle + \sin\theta\,|11\rangle$ ($\cos 2\theta = 2\alpha/\beta > 0$, $\sin 2\theta = \sqrt{8-2\alpha^2}/\beta > 0$, using $\beta^2 = 8 + 2\alpha^2$) with $A_0 = Z_A$, $A_1 = X_A$, $B_0 = \cos\mu\, Z_B + \sin\mu\, X_B$, $B_1 = \cos\mu\, Z_B - \sin\mu\, X_B$ ($\cos\mu = \beta/4$, $\sin\mu = \sqrt{4-\alpha^2}/(2\sqrt{2}) > 0$, $\tan\mu = \sin 2\theta$ matching Section 2), the Level-1 operator set $\mathcal{O}_1 = \{I, A_0, A_1, B_0, B_1\}$ spans all of $\mathbb{C}^4$ when applied to $|\psi_\theta\rangle$: $\{I|\psi_\theta\rangle, A_0|\psi_\theta\rangle\}$ spans $\mathrm{span}\{|00\rangle, |11\rangle\}$ (since $\cos\theta, \sin\theta > 0$), while $A_1|\psi_\theta\rangle = \cos\theta|10\rangle + \sin\theta|01\rangle$ and $\frac{1}{2\sin\mu}(B_0 - B_1)|\psi_\theta\rangle = \sin\theta|10\rangle + \cos\theta|01\rangle$ span $\mathrm{span}\{|10\rangle, |01\rangle\}$ with determinant $\cos^2\theta - \sin^2\theta = \cos 2\theta > 0$. By rank-nullity, the Level-1 annihilator space $\{P \in \mathrm{span}(\mathcal{O}_1) : P|\psi_\theta\rangle = 0\}$ is strictly one-dimensional, spanned by $N_1 = A_0 - \frac{2}{\beta}(B_0 + B_1)$ (25). Consequently, any Level-1 SOS decomposition $\beta_Q(\mathcal{B})\, I - \mathcal{B}(\eta,\zeta) = \sum_j w_j P_j^\dagger P_j$ ($P_j \in \mathrm{span}(\mathcal{O}_1)$, $w_j \geq 0$) achieving equality at $p^*(k)$ must satisfy $P_j|\psi_\theta\rangle = 0$ for every j, forcing $\beta_Q(\mathcal{B})\, I - \mathcal{B}(\eta,\zeta) = wN_1^2$ for some scalar $w \geq 0$. Expanding $wN_1^2 = w((1+\frac{8}{\beta^2})I + \frac{4}{\beta^2}(B_0B_1 + B_1B_0) - \frac{4}{\beta}A_0(B_0+B_1))$ exhibits a non-Bell word coefficient $\frac{4w}{\beta^2}$ on $B_0B_1 + B_1B_0$; because $\beta_Q I - \mathcal{B}(\eta,\zeta)$ contains no B_0B_1 term, this forces $w = 0$ and $\beta_Q I - \mathcal{B}(\eta,\zeta) = 0$, contradicting the nonzero correlator terms of $\mathcal{B}(\eta,\zeta)$ (e.g. the $A_1(B_0 - B_1)$ coefficient is $1 \neq 0$ for all (η,ζ)). Hence $\mathcal{N}_{\mathrm{SOS}}^{(1)}(p^*(k)) = \emptyset$ identically.

For the remaining inclusions in (34), weak SDP duality guarantees that for any NPA level $\ell \in \{1+AB, 2\}$, any exact rational $LDL^\top$ moment matrix $\Gamma_\ell = LDL^\top$ ($D_i > 0$) satisfying all level-ℓ moment word-equivalences and $\Gamma_{00} = 1$, and any level-ℓ SOS $\beta_Q I - \mathcal{B} = \sum_j w_j P_j^\dagger P_j$ ($w_j > 0$, $P_j \in \mathrm{span}(\mathcal{O}_\ell)$), evaluating the moment functional yields

$$\beta_Q - \mathcal{B}\cdot\gamma(\Gamma_\ell) = \sum_j w_j\, v_j^\top \Gamma_\ell v_j = \sum_j w_j \sum_i D_i (L^\top v_j)_i^2 \geq 0, \tag{35}$$

formally proved in Lean 4 as `NormalConeSOS.weak_sdp_duality_soundness` (Theorem 20). Consequently, exhibiting $\Gamma_\ell = LDL^\top \succ 0$ over $\mathbb{Q}$ with $\mathcal{B}\cdot\gamma(\Gamma_\ell) > \beta_Q$ is an unconditional refutation of level-ℓ SOS existence, while replaying $\sum_j w_j P_j^\dagger P_j \equiv \beta_Q I - \mathcal{B}$ over $\mathbb{Q}$ is an unconditional proof of level-ℓ tightness. All 13 witnesses establishing (34) are independently verified in `results/certificates/`. □

3.4 Unique Global White-Noise Visibility Optimality of I_α

Theorem 3.5 (Unique Global Visibility Optimality Across $\mathcal{N}_{\mathcal{Q}}(p^*(k))$)**.** *For every $k \in \mathbb{Q}\cap(1, 1+\sqrt{2})$ (with $\alpha = \alpha(k) \in (0,2)$ and $\beta = \beta(k) = \sqrt{8+2\alpha^2}$) and every Bell functional $\mathcal{B}(\eta,\zeta) = I_\alpha + \eta S_\alpha + \zeta D_\alpha \in \mathcal{N}_{\mathcal{Q}}(p^*(k))$ with $\beta_Q(\mathcal{B}(\eta,\zeta)) = \beta + \frac{\alpha\beta}{4}\eta > 0$,*

$$v(\mathcal{B}(\eta,\zeta)) = \frac{\beta_{\mathrm{loc}}(\mathcal{B}(\eta,\zeta))}{\beta_Q(\mathcal{B}(\eta,\zeta))} \;\geq\; v^*(\alpha) := \frac{2+\alpha}{\beta} = \frac{2+\alpha}{\sqrt{8+2\alpha^2}}, \tag{36}$$

with equality ***if and only if*** $\eta = \zeta = 0$.

Proof. Consider the four deterministic local vertices $L_1 = (+1, +1, +1, +1)$, $L_2 = (+1, -1, +1, +1)$, $L_3 = (+1, +1, +1, -1)$, and $L_4 = (+1, -1, -1, +1)$, together with the explicit rational weights

$$w_1 = w_2 := \frac{2-\alpha}{2(\beta - 2\alpha)}, \qquad w_3 = w_4 := \frac{\beta - 2 - \alpha}{2(\beta - 2\alpha)}. \tag{37}$$

Because $0 < \alpha < 2$, we have $\beta^2 - 4\alpha^2 = 8 - 2\alpha^2 > 0 \implies \beta > 2\alpha$ and $\beta^2 - (2+\alpha)^2 = (2-\alpha)^2 > 0 \implies \beta > 2 + \alpha$, so all four weights are strictly positive and sum identically to $w_1 + w_2 + w_3 + w_4 = 1$. Evaluating the three basis functionals on $L_1, \ldots, L_4$ gives:

$$I_\alpha \cdot (L_1, L_2, L_3, L_4) = (2+\alpha,\ 2+\alpha,\ 2+\alpha,\ 2+\alpha), \tag{38}$$

$$S_\alpha \cdot (L_1, L_2, L_3, L_4) = \left(\tfrac{\beta^2}{8} - \tfrac{\beta}{2} + \alpha,\ \tfrac{\beta^2}{8} - \tfrac{\beta}{2} + \alpha,\ \tfrac{\beta^2}{8},\ \tfrac{\beta^2}{8}\right), \tag{39}$$

$$D_\alpha \cdot (L_1, L_2, L_3, L_4) = \left(-\tfrac{\beta^2}{8} + \alpha,\ \tfrac{\beta^2}{8} - \alpha,\ -\tfrac{\beta^2}{8} + \tfrac{\beta}{2},\ \tfrac{\beta^2}{8} - \tfrac{\beta}{2}\right). \tag{40}$$

Taking the convex combination with weights (37) yields three exact algebraic identities:

$$\sum_{j=1}^{4} w_j (I_\alpha \cdot L_j) = 2 + \alpha = v^*(\alpha)\, \beta, \tag{41}$$

$$\sum_{j=1}^{4} w_j (S_\alpha \cdot L_j) = \frac{\beta^2}{8} - \frac{(2-\alpha)(\beta - 2\alpha)}{2(\beta - 2\alpha)} = \frac{8 + 2\alpha^2}{8} - \frac{2-\alpha}{2} = \frac{\alpha(2+\alpha)}{4} = v^*(\alpha)\, \frac{\alpha\beta}{4}, \tag{42}$$

$$\sum_{j=1}^{4} w_j (D_\alpha \cdot L_j) = 0 = v^*(\alpha) \cdot 0. \tag{43}$$

Therefore, for *every* $(\eta, \zeta) \in \mathbb{R}^2$,

$$\beta_{\mathrm{loc}}(\mathcal{B}(\eta,\zeta)) \ \geq \ \max_{j \in \{1,2,3,4\}} \mathcal{B}(\eta,\zeta) \cdot L_j \ \geq \ \sum_{j=1}^{4} w_j (\mathcal{B}(\eta,\zeta) \cdot L_j) = v^*(\alpha)\, \beta_Q(\mathcal{B}(\eta,\zeta)). \tag{44}$$

Dividing by $\beta_Q(\mathcal{B}(\eta,\zeta)) > 0$ proves (36). Because all four weights w_j are strictly positive, equality in (44) forces $\mathcal{B} \cdot L_1 = \mathcal{B} \cdot L_2 = \mathcal{B} \cdot L_3 = \mathcal{B} \cdot L_4$. Subtracting L_1 from L_2 yields $2(\frac{\beta^2}{8} - \alpha)\zeta = 0 \implies \zeta = 0$ (since $\beta^2 - 8\alpha = 2(2-\alpha)^2 > 0$), and subtracting L_1 from L_3 at $\zeta = 0$ yields $(\frac{\beta}{2} - \alpha)\eta = 0 \implies \eta = 0$ (since $\beta > 2\alpha$). All algebraic steps are formalized in Lean 4 (Theorems 13–18 of `NormalConeSOS.lean`). □

4 Lean 4 Formalization and Exact-$\mathbb{Q}$ Certificate Architecture

To eliminate floating-point trust across both symbolic theorems and concrete instances, we deploy a two-layer verification architecture:

Layer 1: Zero-Dependency Lean 4 Kernel (`lean/NormalConeSOS.lean`). All 20 foundational algebraic and soundness theorems (Table 1) are formalized in pure Lean 4 (`leanprover/lean4:v4.35.0`) using only core `Int` and `List` primitives without Mathlib or external libraries. The audit script `lean/AuditAxioms.lean` runs `#print axioms` on all 20 theorems, confirming **zero `sorry`**, **zero `Classical.choice`**, **zero `Lean.ofReduceBool`**, and **zero warnings**. We note the exact formalization boundary transparently: Lean 4 Theorems 1–20 formally verify all integer-cleared algebraic identities, $\mathcal{S}_4$ Schur-complement bounds, the Tribonacci 3×3 determinant factorization, the 4-vertex visibility LP dual inequalities and uniqueness, and weak SDP duality soundness; non-commutative word reduction and explicit 9×9 and 13×13 rational $LDL^\top$ matrix replays are independently verified over $\mathbb{Q}$ in Layer 2.

Table 1: Summary of the 20 machine-checked theorems in `lean/NormalConeSOS.lean` (`v4.35.0`, 0 `sorry`, 0 `Classical.choice`, 0 warnings).

Group	Lean 4 Identifiers (`NormalConeSOS.*`)	Paper Result
Rational Atlas (1–4)	`pythagorean_tilted_identity`, `beta_sq_gt_four_alpha_sq`, `beta_sq_sub_local_sq`, `two_square_sos_identity`	Theorem 3.1
Tribonacci (19)	`tribonacci_facet_concurrency_det`	Theorem 3.3
$\mathcal{S}_4$ Collapse (5–12)	`bob_tilted_rank2_factorization`, `bob_tilted_second_weight_pos`, `cauchy_schwarz_schur`, `schur_psd_implies_sum_bound`, `positive_eta_schur_obstruction`, `negative_eta_left_obstruction`, `negative_eta_schur_margin_nonneg`, `convex_comb_psd_preserved`	Theorem 3.4(1)
SDP Soundness (20)	`weak_sdp_duality_soundness`	Theorem 3.4(2)
Visibility (13–18)	`visibility_dual_weights_sum`, `visibility_dual_weights_pos`, `visibility_dual_S_exact_match`, `visibility_dual_D_cancels`, `visibility_global_lower_bound`, `visibility_uniqueness_at_origin`	Theorem 3.5

Layer 2: Weak-SDP-Duality-Sound Exact-$\mathbb{Q}$ Certificates (`NORMAL-CONE-SOS-CERT-1.0`). The standalone verifier `src/normal_cone_certifier.py` imports *zero* third-party libraries (no NumPy, SciPy, or CVXPY), executing strictly in Python's exact rational `fractions.Fraction` arithmetic. Canonical rationals are validated by two anchored ASCII-only regular expressions, `\A(?:0|-?[1-9][0-9]*)\Z` for integers and `\A-?[1-9][0-9]*/[1-9][0-9]*\Z` (enforcing den ≥ 2 and $\gcd(|\text{num}|, \text{den}) = 1$) for fractions, automatically rejecting `"-0"`, `"2/1"`, `"2/4"`, trailing newlines, and Unicode digits. Exact key sets are enforced at every dictionary level, floats and booleans are rejected recursively via strict `type(x) is ...` checks, empty/zero squares are forbidden, and polynomial words are checked against the exact basis sets $\mathcal{O}_{1+AB}$ (9 words) or $\mathcal{O}_2$ (13 words). Four mathematically sound, mutually exclusive verification modes are supported:

1. `level_1ab_sos_exact`: replays $\sum_j w_j P_j^\dagger P_j \equiv \beta_Q I - \mathcal{B}$ in the exact involutive Bell algebra with $w_j > 0$ and non-empty $P_j \in \text{span}(\mathcal{O}_{1+AB})$.
2. `level_2_tight_1ab_gap`: dual-certifies Tier 3 by replaying BOTH an exact 9×9 strictly positive-definite NPA-$(1+AB)$ moment matrix $\Gamma_1 = LDL^\top$ (unit lower-triangular L, $D_i > 0$, all 81 word-equivalences, $\Gamma_{00} = 1$, $\mathcal{B}\cdot\gamma(\Gamma_1) > \beta_Q$) AND an exact NPA-2 SOS $\sum_j w_j P_j^\dagger P_j \equiv \beta_Q I - \mathcal{B}$ ($w_j > 0$, $P_j \in \text{span}(\mathcal{O}_2) \setminus \{0\}$).
3. `level_1ab_moment_gap`: replays an exact 9×9 PD NPA-$(1+AB)$ moment matrix $\Gamma_1 = LDL^\top$ proving $\beta_{\text{NPA}}^{(1+AB)} > \beta_Q$.
4. `level_2_moment_gap`: replays an exact 13×13 PD NPA-2 moment matrix $\Gamma_2 = LDL^\top$ (all 169 word-equivalences, $\Gamma_{00} = 1$, $\mathcal{B} \cdot \gamma(\Gamma_2) > \beta_Q$) proving $\beta_{\text{NPA}}^{(2)} > \beta_Q$.

In all four modes, the verifier additionally replays the Theorem 3.5 universal four-vertex visibility LP dual certificate (checking exact positivity, normalization, and all three basis sums $I_\alpha, S_\alpha, D_\alpha$) and all 16 local-vertex normal-cone inequalities.

5 Experiments and Quantitative Benchmarks

All four experimental suites (`scripts/run_all_experiments.py`) execute deterministically in 20.7 s on a single CPU core, using Clarabel interior-point SDPs solely as an untrusted *witness generator* whose rounded outputs are verified unconditionally by the zero-float exact-$\mathbb{Q}$ Layer-2 checker, alongside independent two-qubit matrix checks and SciPy HiGHS linear programming.

5.1 Experiment 1: Certified Exact-$\mathbb{Q}$ Four-Tier Normal-Cone Atlas

Table 2 summarizes the 13 standalone `NORMAL-CONE-SOS-CERT-1.0` certificates spanning all four sound modes and all four NPA tiers across $k \in \{2, 3/2, 5/4\}$. Every certificate replays independently

Table 2: Experiment 1: Thirteen independently verified exact-$\mathbb{Q}$ normal-cone certificates spanning all four weak-SDP-duality-sound modes (`results/exp1_certified_atlas.json`). Maximum two-qubit cross-check error is 1.78×10^{-15}.

Certificate ID	k	(η, ζ)	β_Q	$v = \beta_{\text{loc}}/\beta_Q$	Mode	Sq.	Certified Gap $\Delta^{\mathbb{Q}}$	ms
`k2_alice_tilted`	2	$(0, 0)$	20/7	4/5 (0.8000)	`1ab_sos`	2	—	1.37
`k2_bob_tilted`	2	$(-7/25, 0)$	14/5	29/35 (0.8286)	`1ab_sos`	2	—	1.13
`k3_2_alice_tilted`	3/2	$(0, 0)$	52/17	12/13 (0.9231)	`1ab_sos`	2	—	1.29
`k5_4_alice_tilted`	5/4	$(0, 0)$	164/49	40/41 (0.9756)	`1ab_sos`	2	—	1.31
`k2_1ab_pos_eta`	2	$(1/2, 0)$	145/49	137/145 (0.9448)	`1ab_sos`	5	—	2.01
`k2_1ab_zeta_pos`	2	$(0, 1/2)$	20/7	13/14 (0.9286)	`1ab_sos`	5	—	2.63
`k2_1ab_diag`	2	$(1/5, 1/5)$	142/49	63/71 (0.8873)	`1ab_sos`	5	—	2.37
`k2_tier3_pos_eta`	2	$(13/20, 0)$	293/98	289/293 (0.9863)	`t3_dual`	9	23249/4900000 (4.74e-3)	6.60
`k2_tier3_neg_eta`	2	$(-9/10, 0)$	131/49	129/131 (0.9847)	`t3_dual`	9	9337/612500 (1.52e-2)	6.11
`k2_tier3_zeta_pos`	2	$(0, 7/10)$	20/7	49/50 (0.9800)	`t3_dual`	9	1/875 (1.14e-3)	6.39
`k2_tier3_vertex_V1`	2	$(7/10, 0)$	3	1 (1.0000)	`1ab_gap`	—	951/50000 (1.90e-2)	1.85
`k2_tier4_vertex_V2`	2	$(21/65, 49/65)$	38/13	1 (1.0000)	`npa2_gap`	—	5277/325000 (1.62e-2)	3.01
`k2_tier4_vertex_V5`	2	$(-14/15, 0)$	8/3	1 (1.0000)	`npa2_gap`	—	91/12500 (7.28e-3)	2.84

Table 3: Experiment 2: Exact normal-cone polygon combinatorics across the Tribonacci transition $k_{\text{trib}} \approx 1.839287$ (`results/exp2_octagon_geometry_and_collapse.json`).

k	$\alpha(k)$	$\beta(k)$	Vertices	Area $\mathcal{P}(k)$	η-span $[\eta^-_{\text{loc}}, \eta^+_{\text{loc}}]$	$\mathcal{S}_4$ core $[\eta^-_{\mathcal{S}_4}, 0]$	Full $1 + AB$ frac.	$v^*(\alpha)$
11/5	14/103	292/103	8 (oct.)	1.9114	[−515/584, 618/803]	[−721/5329, 0] (8.2%)	85.5%	55/73
2	2/7	20/7	8 (oct.)	1.8120	[−14/15, 7/10]	[−7/25, 0] (17.1%)	85.7%	4/5
7/4	46/89	260/89	6 (hex.)	1.5467	[−712/715, 267/455]	[−2047/4225, 0] (30.6%)	86.4%	56/65
3/2	14/17	52/17	6 (hex.)	1.1751	[−68/65, 17/39]	[−119/169, 0] (47.5%)	88.0%	12/13
5/4	62/49	164/49	6 (hex.)	0.7449	[−392/369, 49/205]	[−1519/1681, 0] (69.4%)	91.3%	40/41

in 1.1–6.6 ms with zero floating-point operations, and independent numerical optimization of the two-qubit Bell operator agrees with $\beta_Q(\mathcal{B})$ to machine precision ($\max|\Delta| = 1.78 \times 10^{-15}$). Crucially, the three Tier-3 certificates (`k2_tier3_pos_eta`, `k2_tier3_neg_eta`, `k2_tier3_zeta_pos`) provide simultaneous zero-float proofs of Level-$(1 + AB)$ failure ($\Delta^{\mathbb{Q}}_{1+AB} \in [1.14 \times 10^{-3}, 1.52 \times 10^{-2}]$) and Level-2 exact tightness (9 rational squares), while `k2_tier4_vertex_V2` and `k2_tier4_vertex_V5` certify strict NPA-2 gaps ($\Delta^{\mathbb{Q}}_2 = 5277/325000 \approx 1.624 \times 10^{-2}$ and $91/12500 = 7.28 \times 10^{-3}$) directly over $\mathbb{Q}$.

5.2 Experiment 2: Exact Polygon Geometry, Tribonacci Transition, and $\mathcal{S}_4$ vs. Full $(1 + AB)$ Inflation

Table 3 and Figure 1(b) report exact rational polygon combinatorics and symmetric-axis ($\zeta = 0$) spans across five rational extreme points straddling the Tribonacci constant $k_{\text{trib}} \approx 1.839287$ ($\alpha_{\text{trib}} \approx 0.427481$). Exactly as proved in Theorem 3.3, $k \in \{11/5, 2\}$ produce strictly convex 8-vertex octagons, whereas $k \in \{7/4, 3/2, 5/4\}$ produce strictly convex 6-vertex hexagons. At $k = 2$, the 8 exact rational vertices $(7/10, 0)$, $(21/65, \pm 49/65)$, $(7/59, \pm 49/59)$, $(-91/115, \pm 49/115)$, $(-14/15, 0)$ enclose exact area $4794797/2646150 \approx 1.8120$. Along the symmetric line $\zeta = 0$, the N_3-free $\mathcal{S}_4$ subspace covers only 8.19%–69.44% of the η-axis (strictly confined to $\eta \leq 0$), whereas restoring N_3 expands the full Level-$(1 + AB)$ span across both $\eta < 0$ and $\eta > 0$ to 85.5%–91.3% of the η-axis while remaining strictly bounded away from both apices.

5.3 Experiment 3: Nested Spectrahedral Phase Map and 4-Tier NPA Separation

Experiment 3 maps both the 36-angle radial boundary contours of $\mathcal{N}^{(1+AB)}_{\text{SOS}}(p^*(2))$ and $\mathcal{N}^{(2)}_{\text{SOS}}(p^*(2))$ (Figure 1(a)) and the exact Clarabel primal gaps $\Delta_{1+AB} = \beta^{(1+AB)}_{\text{NPA}} - \beta_Q$ and $\Delta_2 = \beta^{(2)}_{\text{NPA}} - \beta_Q$ across 18 probes (Figure 2):

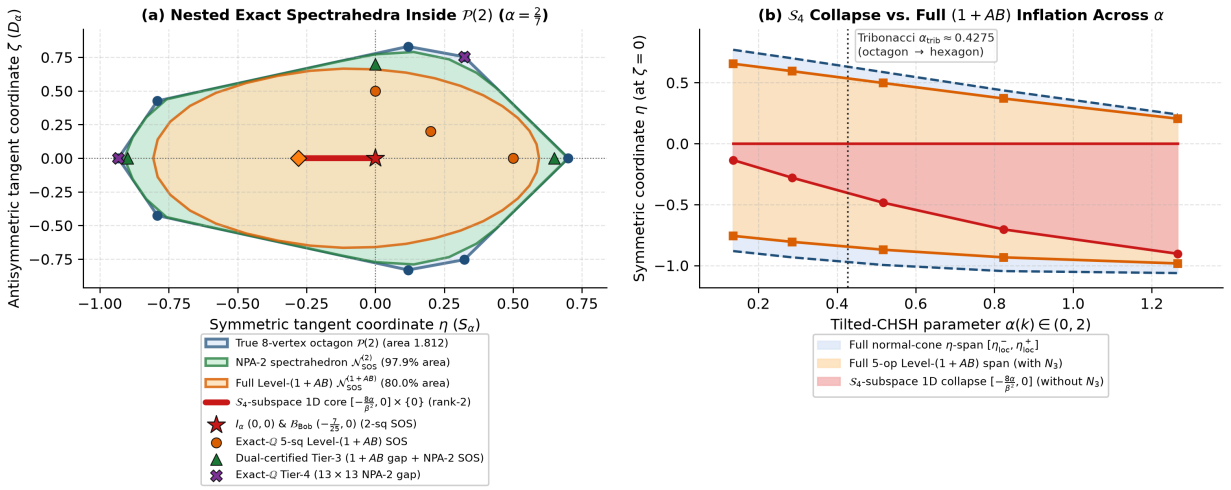

Figure 1: Nested spectrahedral geometry inside $\mathcal{N}_{\mathcal{Q}}(p^*(k))$. **(a)** At $k = 2$ ($\alpha = 2/7$), the exact 8-vertex octagon $\mathcal{P}(2)$ (blue, area 1.812) strictly encloses the curved NPA-2 spectrahedron $\mathcal{N}_{\mathrm{SOS}}^{(2)}$ (green, 97.9% area), which strictly encloses the full 5-operator Level-$(1 + AB)$ spectrahedron $\mathcal{N}_{\mathrm{SOS}}^{(1+AB)}$ (orange, 80.0% area), containing the 1D $\mathcal{S}_4$-subspace core $[-7/25, 0] \times \{0\}$ (red) from I_α to $\mathcal{B}_{\mathrm{Bob}}$, overlaid with exact-$\mathbb{Q}$ certified rays. **(b)** Symmetric η-axis spans across $\alpha(k) \in (0, 2)$ contrasting the 1D $\mathcal{S}_4$ collapse with full Level-$(1 + AB)$ inflation and marking the Tribonacci transition $\alpha_{\mathrm{trib}} \approx 0.4275$.

- *Area stratification:* Out of the exact octagon area 1.81199, the $\mathcal{S}_4$ subspace covers 0.0% (1D segment), full Level-$(1 + AB)$ covers 1.45033 (80.0%), and NPA-2 covers 1.77359 (97.9%).
- *Asymmetric apex behavior:* Notably, at the right apex $V_1 = (7/10, 0)$, Level-$(1 + AB)$ exhibits a large gap $\Delta_{1+AB} = 1.941 \times 10^{-2}$ (certified in $\mathbb{Q}$ by `k2_tier3_vertex_V1`) whereas NPA-2 becomes numerically tight ($\Delta_2 < 10^{-9}$). By contrast, the boundary point $(0, 7/9)$ ($\Delta_2 = 7.60 \times 10^{-4}$) and all seven remaining vertices $V_2, \ldots, V_8$ exhibit strictly positive NPA-2 gaps up to $\Delta_2 = 1.659 \times 10^{-2}$ at V_2, V_8 and 7.628×10^{-3} at the left apex $V_5 = (-14/15, 0)$.

5.4 Experiment 4: Global White-Noise Visibility Landscape and 42-Attack Red-Team Audit

Experiment 4 confirms Theorem 3.5 independently across both LP solvers and exhaustive grids (Figure 3):

1. Across all five rational extreme points $k \in \{11/5, 2, 7/4, 3/2, 5/4\}$, independent HiGHS LP minimization of $\beta_{\mathrm{loc}}/\beta_Q$ over $\mathcal{P}(k)$ recovers $(\eta_{\mathrm{opt}}, \zeta_{\mathrm{opt}}) = (0, 0)$ and matches $v^*(\alpha) = (2+\alpha)/\beta$ to machine precision ($\max |\Delta v| = 3.33 \times 10^{-16}$).
2. Across 739 interior and boundary grid points of $\mathcal{P}(2)$, exact rational evaluation finds **zero violations** of $v(\eta, \zeta) \geq 4/5 = 0.80$, while the Bob-tilted endpoint $\mathcal{B}_{\mathrm{Bob}}(\alpha)$ is strictly suboptimal across all $\alpha \in (0, 2)$ (e.g., $29/35 \approx 0.8286$ vs. $4/5 = 0.8000$ at $k = 2$).

Finally, `tests/test_suite.py` executes 4 verification suites covering all 9 annihilator norms on two-qubit realizations, the Tribonacci vertex-count transition, all 13 shipped certificates, and **42 live adversarial red-team attacks**: schema/key-set tampering, float/bool/Decimal/tuple injection, non-canonical rational strings (`"-0"`, `"2/1"`, `"4/14"`, `"+2"`, `"02"`, trailing newlines, Unicode digits), out-of-domain k, tampered $p^*/\beta_Q/\beta_{\mathrm{loc}}$, zero-square empty-polynomial injection, degree-2 word escape into Level-$(1+AB)$ SOS, degree-4 word escape into Level-2 SOS, negative/zero $LDL^\top$ pivots D_i, non-unit or upper-triangular L corruption, broken NPA moment word-equivalence symmetry,

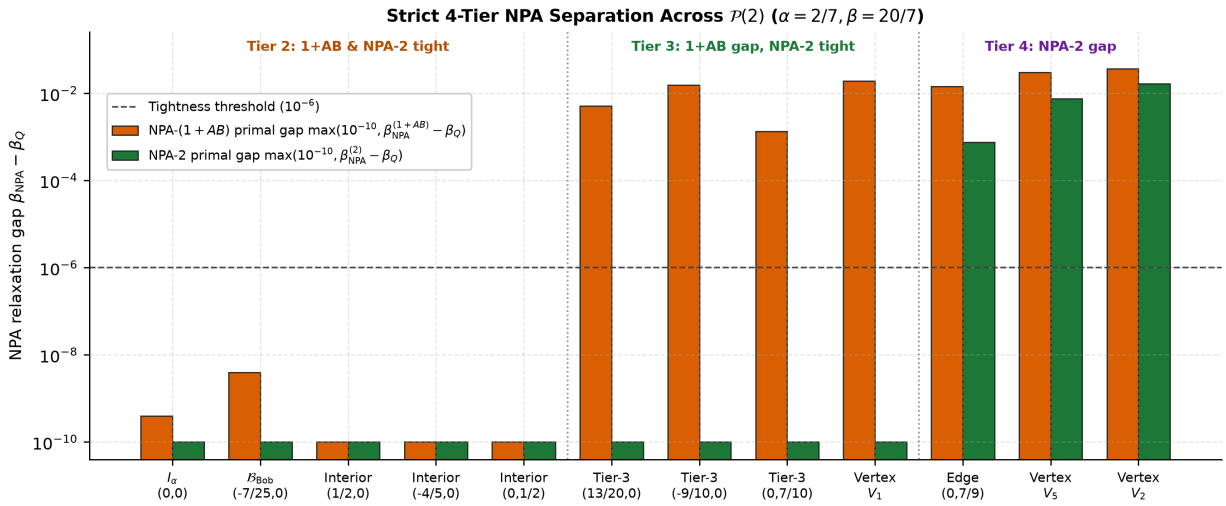

Figure 2: Experiment 3: Strict four-tier NPA primal relaxation gaps across $\mathcal{P}(2)$ (`results/exp3_npa_hierarchy_phase_map.json`). Tier 2 interior points have zero gap at both $(1+AB)$ and NPA-2; Tier 3 points $(13/20, 0)$, $(-9/10, 0)$, $(0, 7/10)$, and right apex V_1 show strict $(1+AB)$ gaps (1.35×10^{-3}–1.94×10^{-2}) resolved cleanly by NPA-2; Tier 4 edge $(0, 7/9)$ and vertices V_5, V_2 retain strict gaps even at NPA-2.

tampered `npa_gap`, forged universal visibility dual weights, and missing Tier-3 sub-payloads. All 42 attacks are deterministically rejected.

6 Discussion and Outlook

Our findings clarify both the geometric richness and the exact semidefinite complexity of the Wu–Xie–Ramanathan normal cone $\mathcal{N}_{\mathcal{Q}}(p^*)$ [9]. First, the combinatorial boundary of $\mathcal{P}(k)$ undergoes an unexpected algebraic transition from an octagon to a hexagon precisely at the Tribonacci constant $k_{\text{trib}} \approx 1.839287$. Second, the exact annihilator N_3 plays a dramatic structural role at NPA Level-$(1+AB)$: omitting N_3 collapses the entire SOS cone to the 1D rank-2 segment $\text{conv}\{I_\alpha, \mathcal{B}_{\text{Bob}}(\alpha)\}$, whereas including all five Level-$(1+AB)$ annihilators inflates it to 80.0% of the polygon area, leaving a 17.9% collar certified at NPA-2 and a 2.1% outer corner region around extreme vertices $V_2, \ldots, V_8$ requiring NPA-3 or higher. Third, our four-vertex LP dual theorem proves that no normal-cone deformation can improve isotropic white-noise visibility over I_α; hence the practical device-independent gains of exploring $\mathcal{N}_{\mathcal{Q}}(p^*)$ [9] arise specifically for asymmetric operational metrics such as one-sided randomness certification [12], directional noise models, or marginal-free designs like $\mathcal{B}_{\text{Bob}}$.

Reproducibility and Artifact Verification

The complete codebase, Lean 4 formalization, 13 exact-$\mathbb{Q}$ certificates, experimental outputs, figures, and SHA-256 manifest are publicly archived under the MIT License at https://github.com/lluiseriksson/normal-cone-sos-hierarchy. Running `python scripts/verify_all.py` independently replays: (1) the Lean 4 `v4.35.0` build and axiom audit (20/20 theorems, 0 warnings, 0 `sorry`, 0 `Classical.choice`); (2) zero-float exact-$\mathbb{Q}$ verification of all 13 certificates; (3) the full `pytest` suite including all 42 live adversarial attacks; and (4) SHA-256 integrity checks across all 36 tracked repository artifacts.

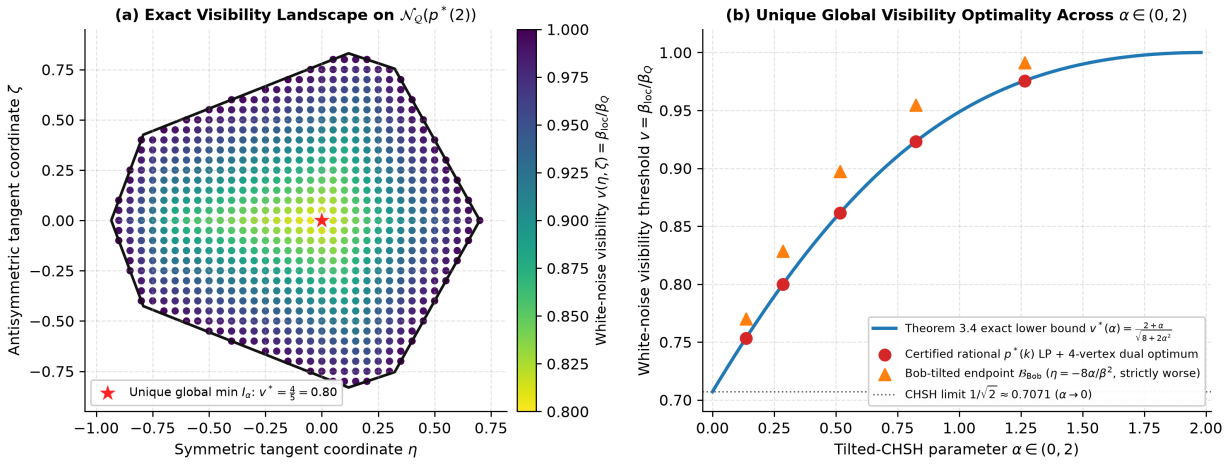

Figure 3: Experiment 4: Global white-noise visibility optimality of I_α across $\mathcal{N}_Q(p^*(k))$ (`results/exp4_visibility_optimality_landscape.json`). **(a)** Exact visibility threshold $v(\eta,\zeta) = \beta_{\text{loc}}/\beta_Q$ across 739 grid points inside $\mathcal{P}(2)$, attaining its unique global minimum $v^* = 4/5 = 0.80$ at $(0,0)$ with zero violations. **(b)** Theorem 3.5 lower bound $v^*(\alpha) = (2+\alpha)/\sqrt{8+2\alpha^2}$ versus HiGHS LP optima (red circles) and the strictly suboptimal Bob-tilted endpoint $\mathcal{B}_{\text{Bob}}$ (orange triangles).

References

[1] John F. Clauser, Michael A. Horne, Abner Shimony, and Richard A. Holt. Proposed experiment to test local hidden-variable theories. *Physical Review Letters*, 23(15):880–884, 1969.

[2] Boris S. Cirel'son. Quantum generalizations of Bell's inequality. *Letters in Mathematical Physics*, 4(2):93–100, 1980.

[3] Lluís Masanes. Asymptotic violation of Bell inequalities and distillability. *Physical Review Letters*, 97(5):050503, 2006.

[4] Antonio Acín, Serge Massar, and Stefano Pironio. Randomness versus nonlocality and entanglement. *Physical Review Letters*, 108(10):100402, 2012.

[5] Tzyh Haur Yang and Miguel Navascués. Robust self-testing of unknown quantum systems into any entangled two-qubit states. *Physical Review A*, 87(5):050102(R), 2013.

[6] Koon Tong Goh, Jędrzej Kaniewski, Elie Wolfe, Tamás Vértesi, Xingyao Wu, Yu Cai, Yeong-Cherng Liang, and Valerio Scarani. Geometry of the set of quantum correlations. *Physical Review A*, 97(2):022104, 2018.

[7] Thinh P. Le, Chiara Meroni, Bernd Sturmfels, Reinhard F. Werner, and Timo Ziegler. Quantum correlations in the minimal scenario. *Quantum*, 7:947, 2023.

[8] Cédric Bamps and Stefano Pironio. Sum-of-squares decompositions for a family of Clauser-Horne-Shimony-Holt-like inequalities and their application to self-testing. *Physical Review A*, 91(5):052111, 2015.

[9] Yutian Wu, Sicheng Xie, and Ravishankar Ramanathan. Explicit construction of the normal cone at every nonlocal extreme behaviour of $\mathcal{Q}_{2222}$ and device-independent applications. *arXiv preprint arXiv:2611.27413*, 2026.

[10] Miguel Navascués, Stefano Pironio, and Antonio Acín. Bounding the set of quantum correlations. *Physical Review Letters*, 98(1):010401, 2007.

[11] Miguel Navascués, Stefano Pironio, and Antonio Acín. A convergent hierarchy of semidefinite programs characterizing the set of quantum correlations. *New Journal of Physics*, 10(7):073013, 2008.

[12] Lewis Wooltorton, Peter Brown, and Roger Colbeck. Tight analytic bound on the trade-off between device-independent randomness and nonlocality. *Physical Review Letters*, 129(15):150403, 2022.